Computer Simulation of Paratrooper Deployment by Static Line from A400M

F.-Javier Mariscal-Sánchez, Sergio Cid-Arroyo, Stephan Priebe
EADS-CASA, Military Transport Aircraft Division
28906, Pº John Lenon, s/n
Getafe (Madrid)
Spain

Javier.Mariscal@casa.eads.net; Sergio.Cid.External@casa.eads.net

ABSTRACT

A computer simulation with the capability to predict paratrooper deployment is presented. The deployment process is split into three phases, which are analyzed using different theoretical approaches. A finite-element approach is used to simulate the bowing of the parachute under the aerodynamic loads, which occurs during extraction from the deployment bag. Canopy inflation is modeled by the semi-empirical Pflanz-Ludtke method. The results obtained agree well with photographic and video data of actual paratroop jumps. To model deployment within the non-uniform flow field around the A400M, a methodology that makes use of data from wind tunnel tests and CFD calculations is proposed. The corresponding simulations are used to analyze the risk of "crossover" – a potentially lethal condition, where paratroopers are drawn towards the centerline behind the aircraft.

1. INTRODUCTION

Like most existing military transport aircraft, the A400M will perform paratrooper airdrops (Figure 1). On existing aircraft, such airdrops are strictly regulated to ensure the safety of the aircraft and the paratrooper. Type-specific rules and procedures apply, and airdrops have to be performed at certain, well-defined aircraft configurations. Traditionally, these procedures and configurations are determined during flight testing once all airworthiness issues have been sorted out. It has long been recognised and documented that this modus operandi is not ideal. Problems, which surface during flight testing, often require complex and expensive fixes. A ready-to-use theoretical model is needed to complement the empirical methods by identifying potential airdrop problems at an early development stage, where design modifications are comparatively easy, quick and cheap. Up to now however, the absence of such a theoretical model has left engineers with no choice but to continue along the stony path of extensive flight testing.

The example of the McDonnel Douglas/Boeing C-17 illustrates how costly and time-intensive the empirical approach can become [1]. During C-17 flight testing, it was identified the possibility of "crossover", a highly dangerous phenomenon where paratroopers exiting from opposite sides of the aircraft are drawn towards the aircraft centreline. Crossover can lead to paratrooper collision and/or parachute entanglement, both of which are potentially lethal. McDonnel Douglas was forced to embark on a very lengthy and expensive wind tunnel and flight testing campaign to reduce the risk of crossover to an acceptable level. Eventually, after a significant testing and engineering effort, the way was paved for certification of the C-17 for mass paratroop jumps.

Mariscal-Sánchez, F.-J.; Cid-Arroyo, S.; Priebe, S. (2006) Computer Simulation of Paratrooper Deployment by Static Line from A400M. In *Fluid Dynamics of Personnel and Equipment Precision Delivery from Military Platforms* (pp. 3-1 – 3-22). Meeting Proceedings RTO-MP-AVT-133, Paper 3. Neuilly-sur-Seine, France: RTO. Available from: http://www.rto.nato.int/abstracts.asp.

Report Documentation Page

Form Approved
OMB No. 0704-0188

1. REPORT DATE	2. REPORT TYPE	3. DATES COVERED
01 OCT 2006	**N/A**	**-**

4. TITLE AND SUBTITLE	5a. CONTRACT NUMBER
Computer Simulation of Paratrooper Deployment by Static Line from A400M	5b. GRANT NUMBER
	5c. PROGRAM ELEMENT NUMBER
6. AUTHOR(S)	5d. PROJECT NUMBER
	5e. TASK NUMBER
	5f. WORK UNIT NUMBER
7. PERFORMING ORGANIZATION NAME(S) AND ADDRESS(ES) **EADS-CASA, Military Transport Aircraft Division 28906, Pº John Lenon, s/n Getafe (Madrid) Spain**	8. PERFORMING ORGANIZATION REPORT NUMBER
9. SPONSORING/MONITORING AGENCY NAME(S) AND ADDRESS(ES)	10. SPONSOR/MONITOR'S ACRONYM(S)
	11. SPONSOR/MONITOR'S REPORT NUMBER(S)

12. DISTRIBUTION/AVAILABILITY STATEMENT
Approved for public release, distribution unlimited

13. SUPPLEMENTARY NOTES
See also ADM202394., The original document contains color images.

14. ABSTRACT

15. SUBJECT TERMS

16. SECURITY CLASSIFICATION OF:			17. LIMITATION OF ABSTRACT	18. NUMBER OF PAGES	19a. NAME OF RESPONSIBLE PERSON
a. REPORT	b. ABSTRACT	c. THIS PAGE			
unclassified	**unclassified**	**unclassified**	**UU**	**22**	

Figure 1: Artist's Impression of Mass Paratroop Jump from A400M

The challenges associated with airdrop computer simulations are substantial because the initial stages of paratrooper deployment are highly dynamic and non-linear. Furthermore, the entire system (paratrooper, parachute, deployment bag and static line) is immersed in the non-uniform flow field generated by the aircraft. Under these conditions, numerical stability is often difficult to achieve.

In this paper, a computer simulation is developed to predict the trajectory of paratroopers during deployment. The procedure, which falls under the engineering model category of the physical simulation hierarchy, contains several modules, which together cover the entire deployment process from the moment when the paratrooper exits the aircraft to full canopy inflation and beyond. Some modules use a single body theoretical model (e.g. straightforward Newtonian trajectory integration to simulate the first jump phase, which begins when the paratrooper exits the aircraft and ends when the static line is stretched). Others, however, use finite-element models (e.g. to simulate the bowing of the parachute under the aerodynamic loads, which occurs while the parachute is being extracted from the D-bag).

Airdrop computer models allow potential risks such as crossover to be identified and addressed at an early stage. As these computer models become increasingly refined in the future, flight testing will play a lesser role in determining paratroop deployment aircraft configurations. Instead, the focus of flight testing will shift towards confirmation, fine-tuning and qualification, thus shortening the testing/certification process and reducing cost.

2. DESCRIPTION OF DEPLOYMENT PROCESS

The static line deployment method, which is standard practice for mass paratroop jumps, is considered here. As its name suggests, this deployment method makes use of a "static line" – a cable, which connects the paratrooper's deployment bag (D-bag) to an anchor point inside the aircraft.

A thorough study of photographic and video evidence [2,3] suggests that the deployment process is made up of three physically distinct phases (Figure 2).

Phase 1. Initial deployment

The first phase starts when the paratrooper exits the aircraft and ends when the static line is stretched. During this phase, the parachute is still undeployed and is stored inside the D-bag on the paratrooper's back. Since the static line is unstretched and exerts negligible force, the body constituted by the parachute, the D-bag and the paratrooper is free-falling under the action of only two forces: its weight and the aerodynamic forces, of which only drag is considered.

Phase 2. Parachute extraction

The second phase starts when the static line is fully-stretched and ends when the parachute is completely extracted from the D-bag. At the beginning of this phase, the fully-stretched static line exerts sufficient force on the D-bag for it to separate from the paratrooper. The D-bag is constrained by the stretched static line while the paratrooper continues to fall away from the aircraft, extracting the parachute – lines first – from the D-bag. The extracted portion of the parachute is not parallel to the wind and bows under the action of the aerodynamic forces. The D-bag is in quasi-equilibrium, constrained by the static line and rises slowly as its mass decreases because of parachute extraction.

Phase 3. Aerodynamic straightening and inflation

The third phase is characterised by aerodynamic cross-flow effects (as in phase 2) and parachute inflation. At the beginning of this phase, the parachute's tip is bent forwards into the flow. However, under the action of the aerodynamic forces, the tip quickly whips backwards. The parachute straightens and adopts a "leant-back" attitude, which is more in-line with the flow. When this configuration is reached, the inflation begins. Due to the inflation effects, the parachute rotates from the leant-back attitude – which may be as leant-back as near-horizontal or horizontal –towards the vertical. This movement continues after fully inflation, when the parachute oscillates and, eventually, stabilises at a certain characteristic descent speed. During this phase the empty D-bag, whose movement is independent of the rest of the parachute and paratrooper, stabilizes at certain position determined by the equilibrium of the gravity, tension of the static line and aerodynamic forces.

Although strictly speaking, the simulation of phase 3 requires a theoretical model, which combines the aerodynamic cross-flow effects with parachute inflation, video evidences [3] suggests that initially the aerodynamic cross-flow effects dominate over inflation and, after some point in time, inflation dominates over the aerodynamic cross-flow effects.

This observation allows to approach the phase 3 by two sub-phases, 3a and 3b. Phase 3a starts when the parachute is fully extracted from the D-bag and goes on as long as aerodynamic cross-flow effects dominate. It is followed by phase 3b, which is dominated by inflation. There is not theoretical model to determinate the moment in time when the focus shifts from aerodynamic cross-flow effects to canopy inflation. This time must be selected trough the study and extrapolation of the existing paratrooper jumps evidences.

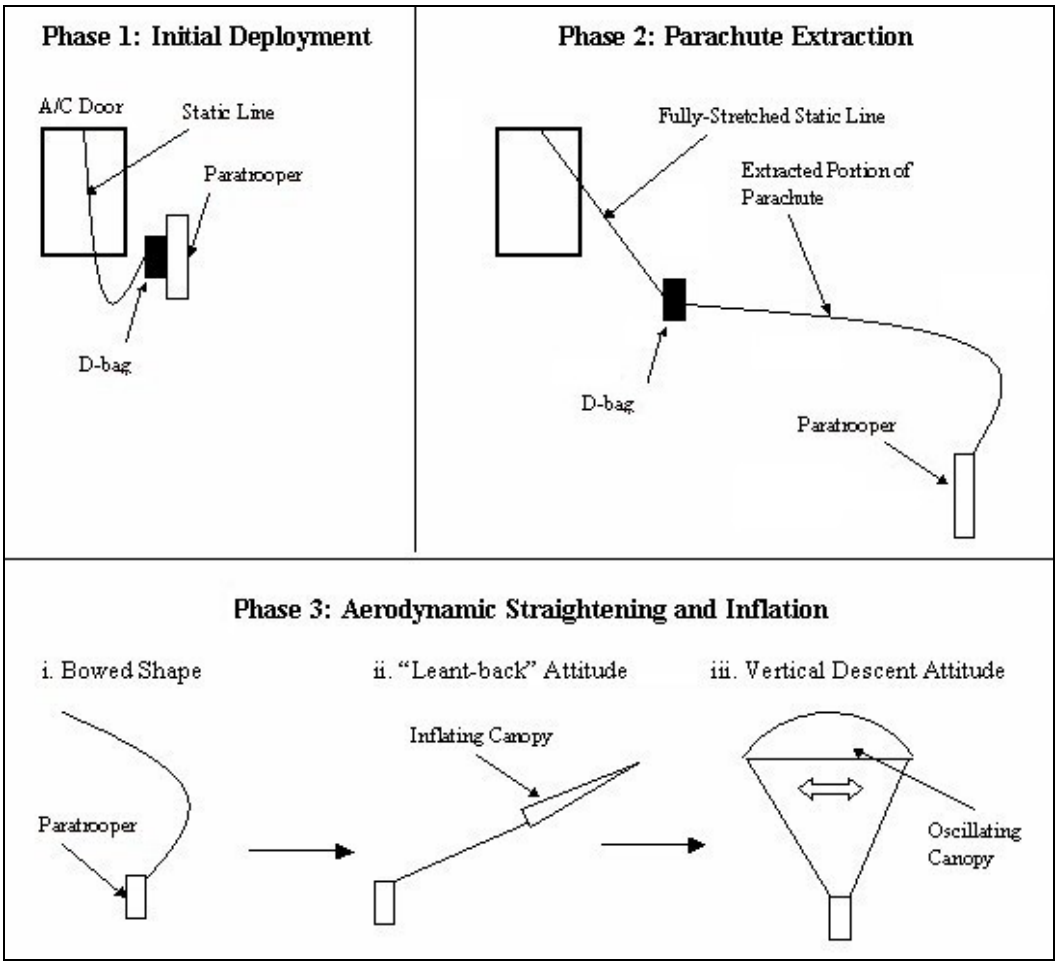

Figure 2: Schematic Representation of the Deployment Process

Using photographic evidence, Accorsi et al. [4] have recently suggested that an additional phase exists between phases 1 and 2. They note that the separation of the D-bag from the paratrooper is not instantaneous but follows a sequence: As the static line is stretched, the lower part of the D-bag (where the static line is attached) separates from the paratrooper while the upper part stays attached. The D-bag then pivots about its upper, attached part before separating fully from the paratrooper. Accorsi et al. estimate that this phase lasts approximately 0.02s. Since this is short compared to the duration of the initial deployment phase (phase 1), which takes approximately 0.7s, and the duration of the extraction phase (phase 2), which also takes approximately 0.7s, the additional "separation-phase" observed by Accorsi et al. has been neglected in the work presented here.

3. THEORETICAL MODELS

Different theoretical models are used to simulate the various phases of the deployment process:

a. Point Mass Model (Phase 1)

During the initial deployment phase, the paratrooper and the D-bag (which contains the parachute) are linked and may be regarded as a single body. To simplify matters further, that single body may be modelled as a point mass, in which case only Newton's force equation needs to be considered. In an aircraft-fixed reference system,

$$m\frac{d^2\vec{r}(t)}{dt^2} = \vec{F}(\vec{r},t) = \vec{F}_{aero} + m\vec{g} \qquad (1)$$

Where m is the mass of the body (which is the sum of the mass of the empty D-bag, the parachute and the paratrooper), $\vec{r}$ is the position of the point mass, t is time and $\vec{F}$ is the force acting on the point mass. Note that the aircraft-fixed reference system is considered to be inertial since the aircraft is usually in steady, level flight while airdropping paratroopers.

As mentioned earlier, the static line exerts negligible force on the D-bag when unstretched, and the force acting on the point mass is thus composed of only two contributions: the weight and the aerodynamic forces. The weight is constant since the mass of the body does not change during the initial deployment phase. The aerodynamic force is simplified to consist only of its drag component, and it may be expressed as follows:

$$\vec{F}_{aero}(\vec{r},t) = \tfrac{1}{2}\rho SC_D \cdot \left|\vec{V}_{aero}(\vec{r},t)\right| \cdot \vec{V}_{aero}(\vec{r},t) \qquad (2)$$

Where ρ is air density, SC_D is the equivalent drag area and $\vec{V}_{aero}$ is the flow velocity with respect to the point mass, which may be expressed as:

$$\vec{V}_{aero}(\vec{r},t) = \vec{V}_{body}(\vec{r},t) - \vec{V}_{FlowField}(\vec{r},t) \qquad (3)$$

Where $\vec{V}_{body}$ is the body velocity relative to the aircraft and $\vec{V}_{FlowField}$ is the flow velocity (at the position $\vec{r}$ of the point mass), which can be derived from CFD calculations, wind tunnel testing or a combination of both, as will be discussed later.

Equation (1), combined with equations (2) and (3), is integrated using an explicit integration scheme, like Runge-Kutta. The scheme order is a function of the desired accuracy and the calculation cost.

The initial position depends of the situation of the lateral doors in the aircraft, whereas for the initial velocity modulus and direction, values within a standard range are selected,

b. Finite-Element Model (Phases 2 & 3a)

A finite-element model is used to simulate the "aerodynamic bowing" of the extracted portion of the parachute during phase 2 and the subsequent "aerodynamic straightening" of the entire, fully extracted non-inflated parachute during phase 3a. The approach presented here owes much to Moog [5] and Purvis [6]. The entire parachute system (made up of the canopy, the suspension lines and the paratrooper) is

modelled as a series of discrete mass nodes, linked by massless, straight segments (Figure 3). The structural and aerodynamic loads, which act on the segments, are directly applied at the nodes.

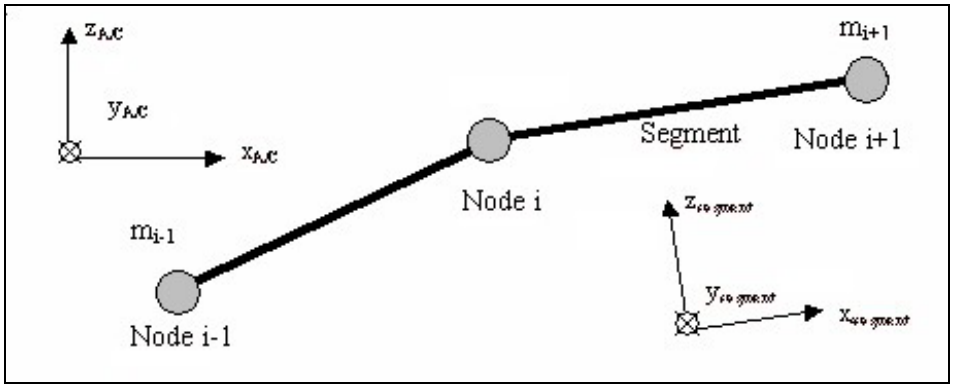

Figure 3: Schematic Representation of the Finite-Element Model

During phase 2, the number of employed nodes increase as the lines and canopy are being extracted. Consequently, the mass of the node representing the D-bag decreases.

Structural Loads

The mass nodes are elastically linked, and the tension between two nodes is given by a linear stress-strain relationship (Hooke's law), complemented by a first-order linear damping term. In segment fixed co-ordinates (x-direction *along* the segment):

$$\vec{T} = \begin{pmatrix} EA\varepsilon + B\dot{\varepsilon} \\ 0 \\ 0 \end{pmatrix} \qquad (4)$$

Where E is Young's modulus, A is the cross-sectional area of the segment linking two nodes, ε is the strain in the segment, B is a damping parameter (see Moog [5]), and $\dot{\varepsilon}$ is the strain rate, $d\varepsilon/dt$. Compression in the segments is not allowed, as this would be unphysical.

The segments representing the lines as well as the uninflated canopy are idealised as rods. The geometrical and mechanical characteristics of these rods – such as the cross-sectional area, A, or Young's modulus, E – depend on the parachute type under consideration.. Typical values of these properties are readily available in published databases or papers (e.g. Knacke [7]).

Aerodynamic Loads

The aerodynamic loads are made up of two components: an axial component, which is supposed to consist solely of skin-friction drag, and a normal component, which consists of cross-flow drag. In segment-fixed co-ordinates, the skin friction drag is given by:

$$\vec{F}_{SkinFriction} = \tfrac{1}{2}\rho S C_f \cdot \vec{V}_{axial} \cdot \left|\vec{V}_{axial}\right| \qquad (5)$$

Where ρ is the local air density, S is the wetted area, C_f is the skin-friction coefficient and $\vec{V}_{axial}$ is the

flow velocity in the axial direction of the segment. The lines and the uninflated canopy are idealised as rods, and the wetted area of a segment thus corresponds to the product of the segment circumference and its length. Standard expressions for the skin-friction coefficient are used (see [8]).

The cross-flow drag (normal aerodynamic force) is of the form:

$$\vec{F}_{CrossFlow} = \tfrac{1}{2}\rho S C_D \cdot \vec{V}_{normal} \cdot \left|\vec{V}_{normal}\right| \qquad (6)$$

Where ρ is the local air density, S is the reference area, C_D is the drag coefficient and $\vec{V}_{normal}$ is the flow velocity normal to the segment. The reference area corresponds to the segment planform area, i.e. the product of the segment diameter and its length. As mentioned earlier, the lines as well as the uninflated canopy are bunched together, roughly forming a circular cylinder. Therefore, the drag coefficient for a two-dimensional cylinder is used, for instance $C_D \approx 1$ [9].

The total aerodynamic force is the sum of the axial and normal components. In segment-fixed co-ordinates:

$$\vec{F}_{aero} = \vec{F}_{axial} + \vec{F}_{normal} = \vec{F}_{SkinFriction} + \vec{F}_{CrossFlow} \qquad (7)$$

Equation of Motion of a Node

The nodes have three degrees of freedom each and their translational motion is governed by Newton's force equation, which is of the following form (for the i^{th}-node):

$$m_i \frac{d^2 \vec{r}_i}{dt^2} = m_i \vec{g} + \vec{T}_{i+1} - \vec{T}_i + \vec{F}_{aero_i} \qquad (8)$$

Where m_i is the node mass, $\vec{r}_i$ is the node position in aircraft co-ordinates, $\vec{g}$ is the gravity vector, $\vec{T}_{i+1}$ is the tension in the segment between nodes i and i+1, $\vec{T}_i$ is the tension in the segment between nodes i-1 and i and $\vec{F}_{aero_i}$ is the resultant of the aerodynamics over the i^{th} node now exposed in aircraft coordinates.

c. Inflation Model (Phase 3b)

Canopy inflation is a highly dynamic and non-linear process, which is very difficult to simulate. There is a wealth of semi-empirical inflation models [7], which often require considerable user input and only apply to a restricted set of cases. Although the program permits the implementation of any of these semi-empirical models or the use of experimental data, the Pflanz-Ludtke method, which is the most common inflation model, is selected for the present work. This model assumes that, during inflation the variation of drag area with time is only dependent of the parachute/canopy type, but independent of initial velocity, altitude, canopy dimensions etc. The variation of drag area with time is given by:

$$SC_D(t) = \left(SC_{Df} - SC_{D0}\right)\left(\frac{t - t_0}{t_{\inf}}\right)^6 + SC_{D0} \qquad (9)$$

Where $SC_D(t)$ is the drag area at time t, SC_{D0} is the initial drag area prior to inflation, SC_{Df} is the fully inflated parachute drag area, t_{inf} is the inflation time and t_0 is the start inflation time.

Usually, the values of SC_{D0} and SC_{Df} are supplied by parachute manufacturer, which obtain the data by experimental test. If this way is not this possible, the values of SC_D for typical parachute models can be found in specialized literature [7].

The inflation time can be estimated as [10]:

$$t_{\inf} = \frac{nD_0}{V_s} \qquad (10)$$

Where n is a dimensionless parameter, which is characteristic of a given parachute type, D_0 is the nominal diameter and V_s is the so-called "snatch-velocity", i.e. the velocity at line-stretch when the snatch-force occurs. The parameter n can be estimated from test data. Furthermore, a certain number of empirical approximations exist for common parachute models, like flat-circular canopies [11].

The uncertainties in the determination of V_s and n make it difficult to fix a unique and accurate value for $t_{\inf}$. As small variations of $t_{\inf}$ have significant influence on the inflation process, $t_{\inf}$ is handled as a statistical parameter, with its own mean value and standard deviation.

During inflation, unsteady aerodynamic effects occur, which significantly influence the behaviour/inertia of the canopy. They are accounted for by "added mass"-terms in equation of motion. Cockrell [11] notes that "added mass" is actually a tensor and that cross-components exist, i.e. a certain, arbitrary acceleration along direction A may cause added mass components, which act on forces that are *not* along A, but along some other direction. According to Cockrell, these cross-components may however be neglected, in which case "added mass" is a vector (in 3-DOF). It may be expressed as a function of displaced volume, commonly denoted $\forall$, and of air density, ρ:

$$\bar{a} = \rho \forall \cdot \vec{k} \qquad (11)$$

Where $\vec{k}$ is the vector of "added mass coefficients". The latter are constants for a given body shape and attitude and are usually determined experimentally (refer to Cockrell [11] for an account of the experimental methods employed and a summary of useful numerical data).

The drag area evolution and the added mass vector are referred to a point mass canopy. Several author have modelled the parachute and its payload (paratrooper) as two point masses joined by an elastic link with three degrees of freedom each, and although this approximation permits the qualitative study of the movement, it is not enough accurate for the determination of crossover risk, since the shape of the canopy and suspension lines during the movement are as important as the paratrooper position.

For this reason, the added mass vector and the drag area evolution have been assigned to the canopy nodes. During the inflation, the node added masses vary, and the Newton's force equation for the canopy i^{th}-node is

$$\frac{d^2 m_i \bar{r}_i}{dt^2} = m_i \bar{g} + \vec{T}_{i+1} - \vec{T}_i + \vec{F}_{aero_i} \qquad (12)$$

Where m_i is the sum of the node mass and its added mass, $\bar{r}_i$ is the node position in aircraft co-ordinates, $\bar{g}$ is the gravity vector, $\vec{T}_{i+1}$ is the tension in the segment between nodes i and i+1, $\vec{T}_i$ is the tension in the segment between nodes i-1 and i and $\vec{F}_{aero_i}$ is the resultant of the aerodynamics over the i^{th} node now

exposed in aircraft coordinates, and it takes part of the inflation evolution of drag area.

For the paratrooper, unsteady effects are negligible and Newton's equation applies in the classic form, without added mass. The forces acting on the paratrooper are its weight, the aerodynamic drag, and the tension in the elastic link:

$$\vec{F}_{paratrooper} = m_{paratrooper}\vec{g} + \frac{1}{2}\rho SC_{D\ paratrooper} \cdot \left|\vec{V}_{paratrooper}\right| \cdot \vec{V}_{paratrooper} - \vec{T}_{paratrooper} \qquad (13)$$

Where $\vec{F}_{paratrooper}$ is the force vector in aircraft co-ordinates, $m_{paratrooper}$ is the paratrooper's mass, $SC_{D\ paratrooper}$ is the paratrooper drag area (which depends on the paratrooper's anatomy, attitude etc), $\vec{V}_{paratrooper}$ is the flow velocity relative to the paratrooper in aircraft co-ordinates (equivalent to equation (3)) and $\vec{T}_{paratrooper}$ is the tension force between the paratrooper and the first suspension lines node.

The empty D-bag movement is determined by the Newton's force equation:

$$\vec{F}_{D-Bag} = m_{D-Bag}\vec{g} + \frac{1}{2}\rho SC_{D\,D-Bag} \cdot \left|\vec{V}_{D-Bag}\right| \cdot \vec{V}_{D-Bag} - \vec{T}_{D-Bag} \qquad (14)$$

Where $\vec{F}_{D-Bag}$ is the force vector in aircraft co-ordinates, m_{D-Bag} is the paratrooper's mass, SC_D is the paratrooper drag area (which depends on the paratrooper's anatomy, attitude etc), $\vec{V}_{D-Bag}$ is the flow velocity relative to the paratrooper in aircraft co-ordinates (equivalent to equation (3)) and $\vec{T}_{D-Bag}$ is the tension force between D-bag and aircraft anchor point.

4. A400M FLOW FIELD MODEL

To model deployment within the non-uniform flow field around the A400M, a methodology that makes use of data from experiments and CFD calculations is used. This methodology takes into account the effect of the flow field on the paratrooper, but not, inversely, the effect of the paratrooper on the flow field. The near field is derived from wind tunnel testing. A flow survey (Figures 4 and 5) using a rake of 5-hole probes was performed on a powered (live propellers) model of the A400M aircraft (FLA4.3 model, scale 1:15) in RUAG low speed wind tunnel in Emmen (Switzerland). During these tests, flow velocity components and dynamic pressure were measured on planes perpendicular to fuselage (Figures 6 and 7). The far field data is obtained by means of a CFD calculation using an Euler code. To assure a smooth transition between wind tunnel tests and CFD data at each measured plane a fading scheme was used.

Although the extraction of flow information at any point of space is cheap for already converged CFD calculations, this is not true with experimental data. Wind tunnel tests are expensive and flow surveys are highly time-consuming, so reducing the number of surveying planes to a minimum is desirable. Once each of these wind tunnel data planes is extended with CFD data, a flow-feature-keeping interpolation methodology is employed to improve spatial resolution between these planes without the need for costly extra measuring planes on wind tunnel. This interpolation scheme correlates different flow features (such as vortex cores) between planes to obtain data at intermediate position tracking the evolution of the selected flow features, avoiding duplicity of them. Differences with a standard interpolation can be seen on Figure 8, where duplicity of features is evident.

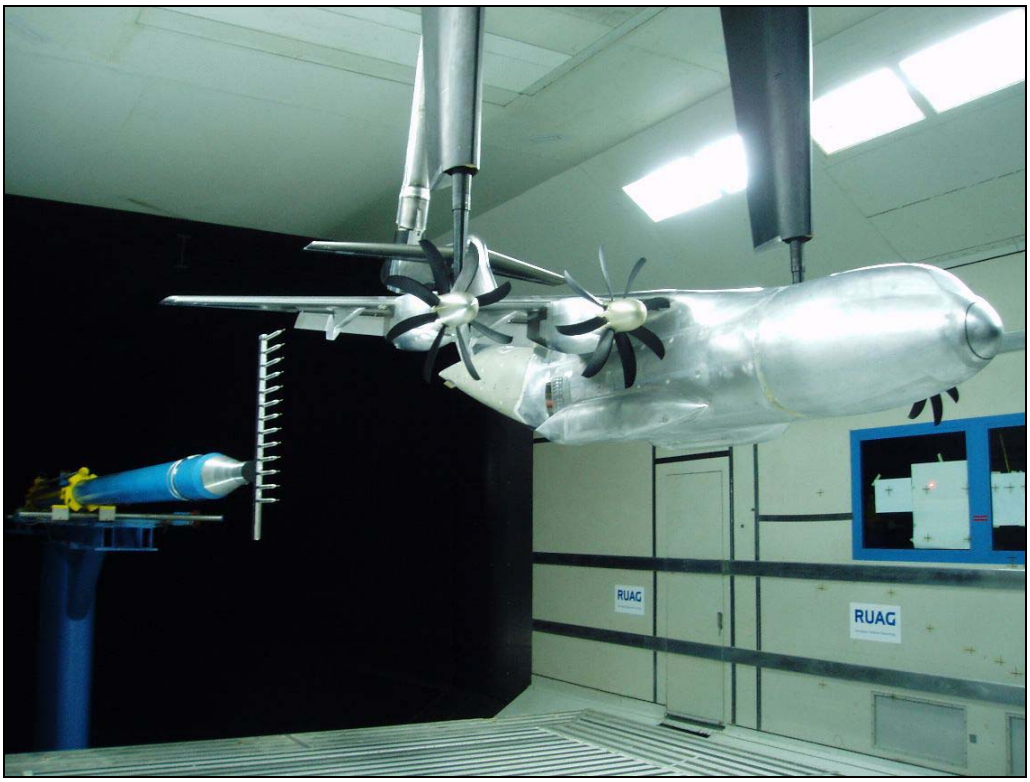

Figure 4: Flow survey in A400M wind tunnel model

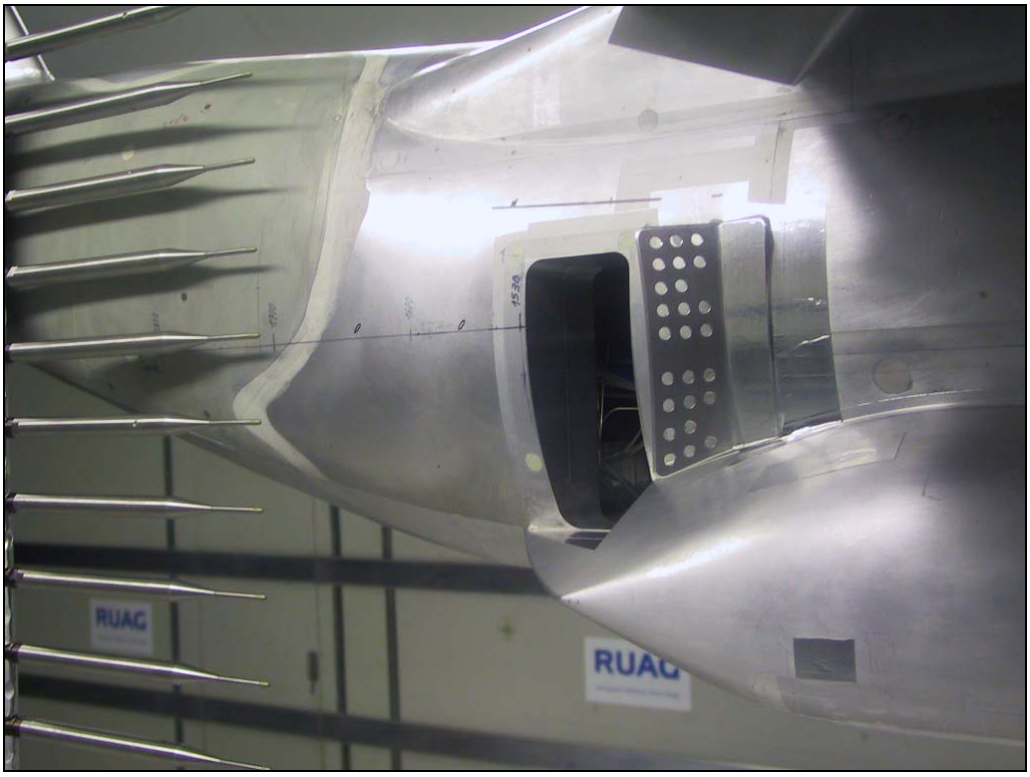

Figure 5: Flow survey detail in A400M wind tunnel model

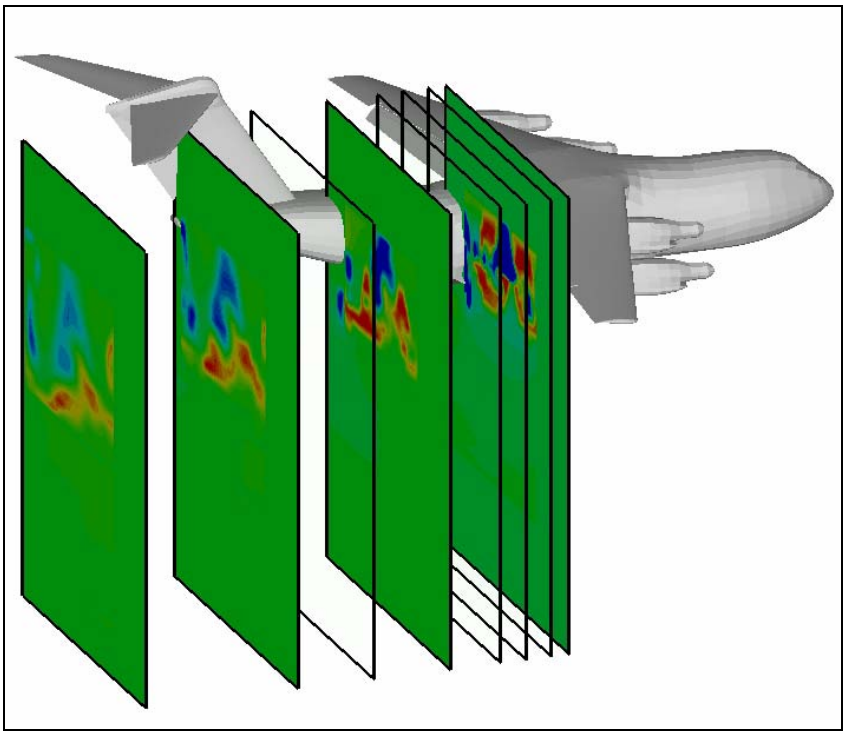

Figure 6: Flow survey measurement planes in A400M wind tunnel model (for some planes only the boundary is represented for clarity)

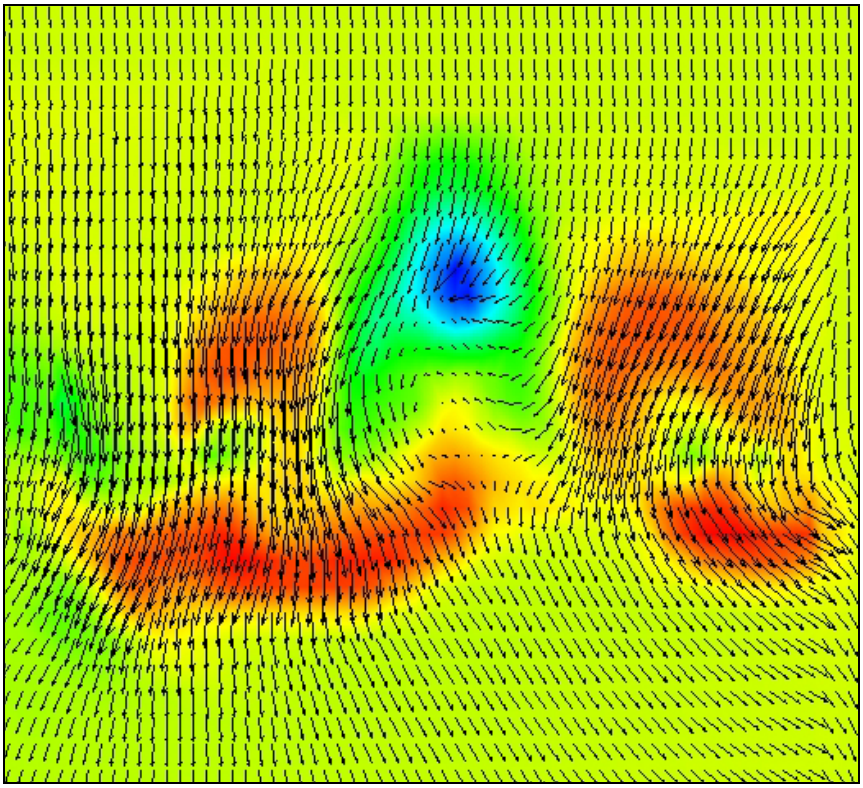

Figure 7: Example of flow survey results. Contour: Vx. Vector representing Vy and Vz

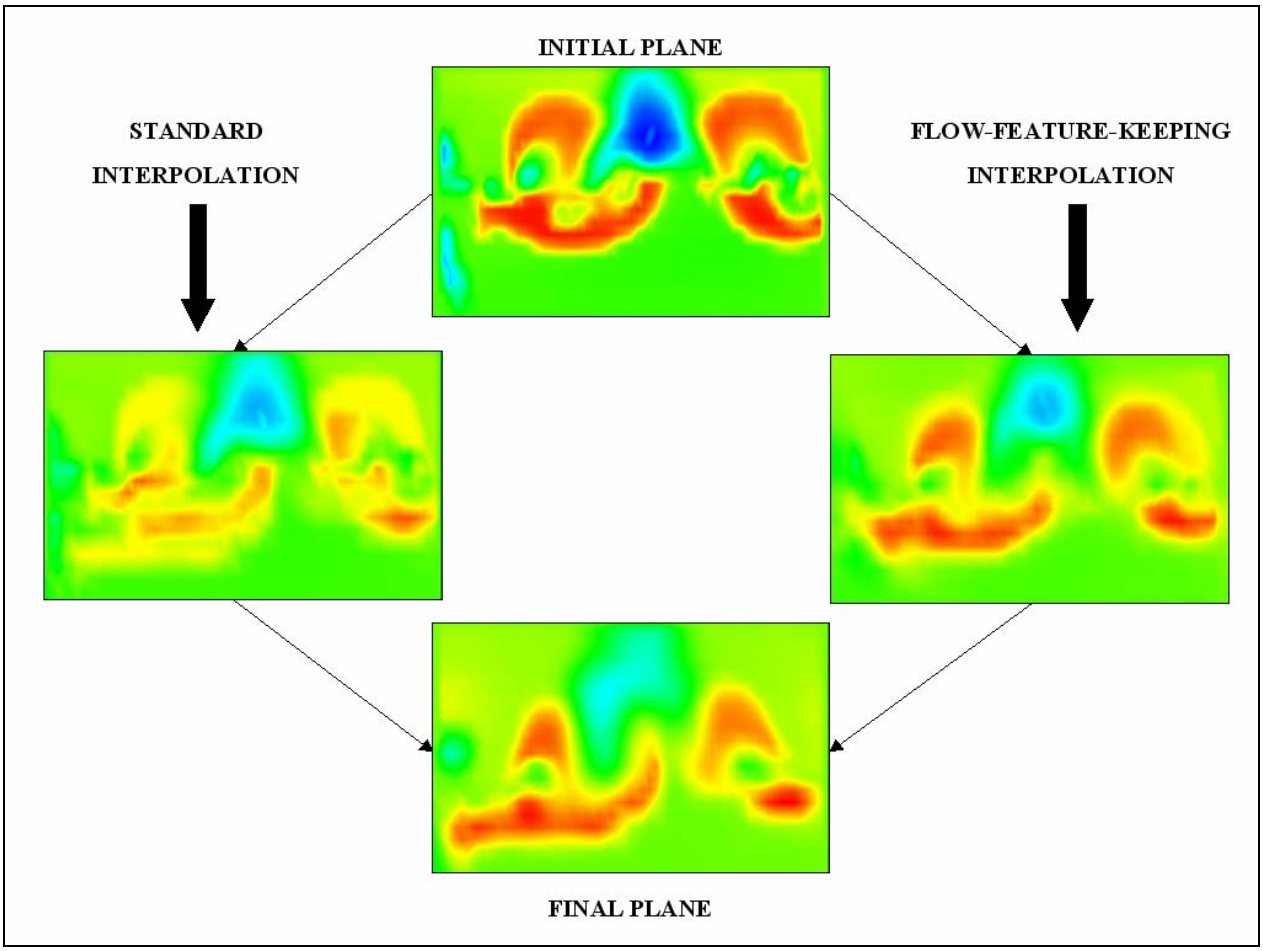

Figure 8: Interpolation method comparison. Dynamic pressure contours

5. RESULTS

The point mass model, the finite-element model and the inflation model constitute a unique program, which may be executed directly to simulate the entire deployment process.

A standard ODE solver routine, based on a Runge-Kutta scheme, is used to integrate the movement equations. The selection of the desired integration scheme is a function of the necessary accuracy and the calculation effort limitations.

Problems with numerical stability, which are due to the highly dynamic and non-linear nature of the underlying physical phenomena, have been encountered when running the program, especially during the parachute extraction phase.

These instabilities have been encountered as well by other authors, as reported for example by Accorsi et al [4]. They recommend introducing numerical damping, since it retains the physically important low frequency behaviour while removing the destabilising high frequency behaviour. Following this argument, damping has been used in the program presented here, and this has indeed proven to be a successful measure in improving stability.

A series of results for a jump of a 150 kg paratrooper with initial velocity of 1 m/s in a flow field corresponding to a typical 1g air delivery condition are given in figures 9 to 23. Visual comparison with photographic and video data [2, 3] shows close agreement between the predicted and actual shapes of the parachute, although further and more thorough validation of the results is required.

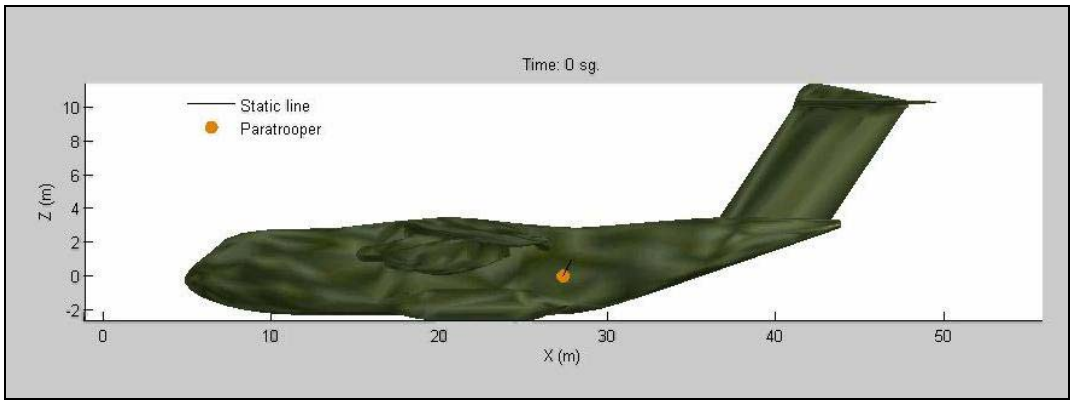

Figure 9: Jump initial conditions

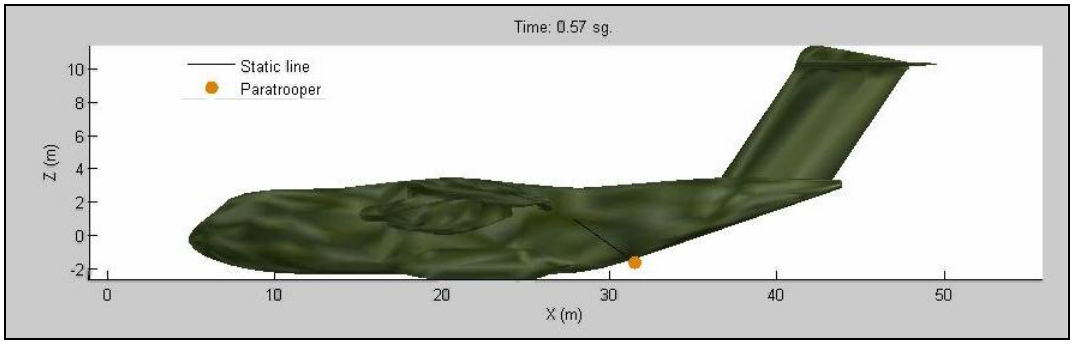

Figure 10: Static line full strechted

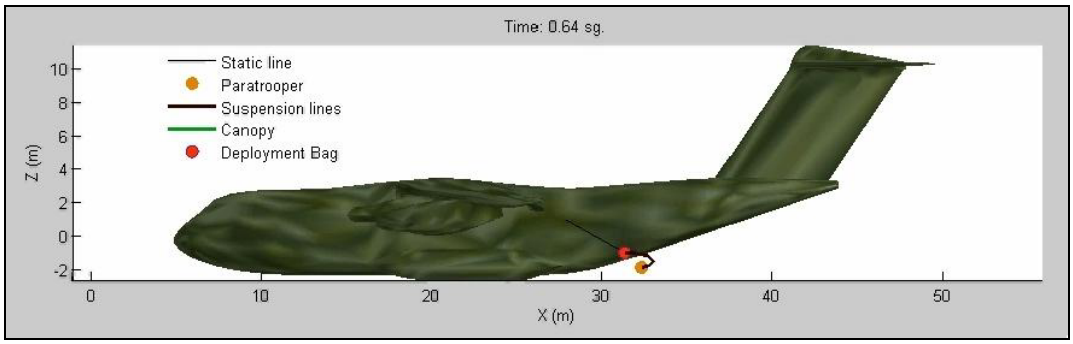

Figure 11: Parachute deployment (I)

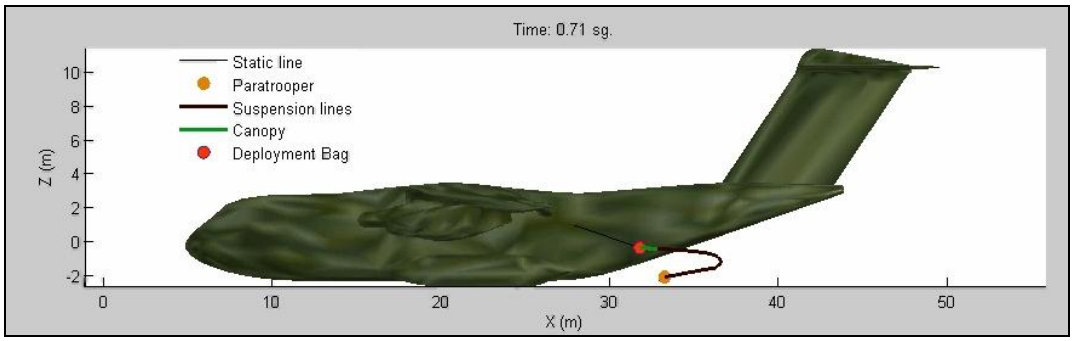

Figure 12: Parachute deployment (II)

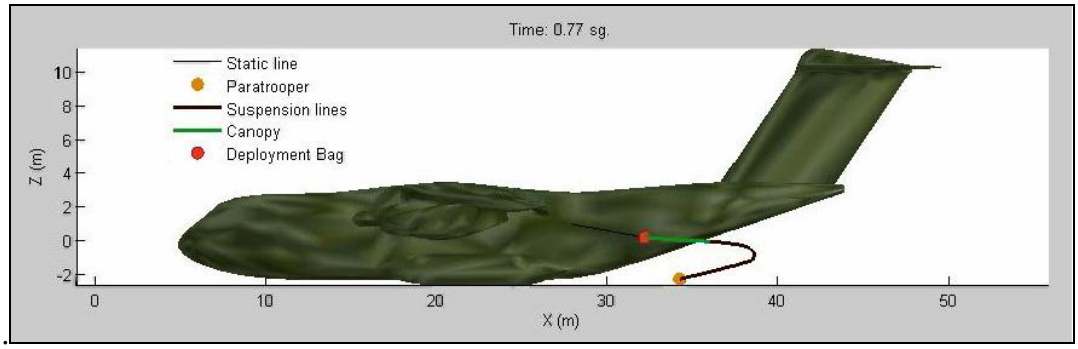

Figure 13: Parachute full deployed

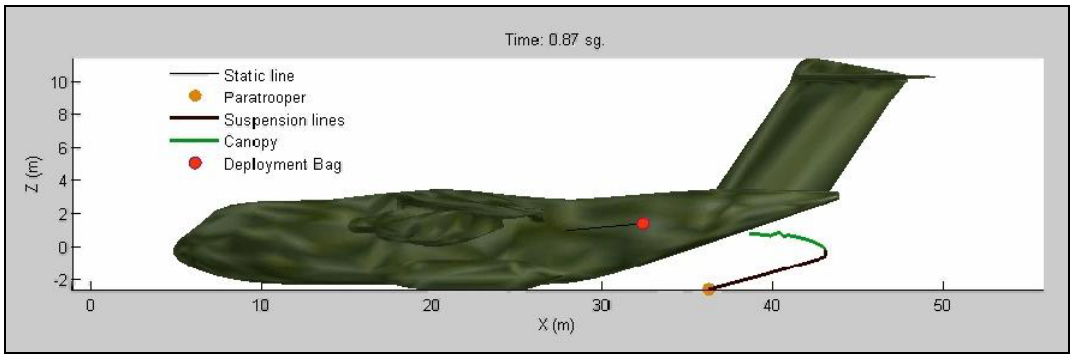

Figure 14: Cross flow effects phase (I)

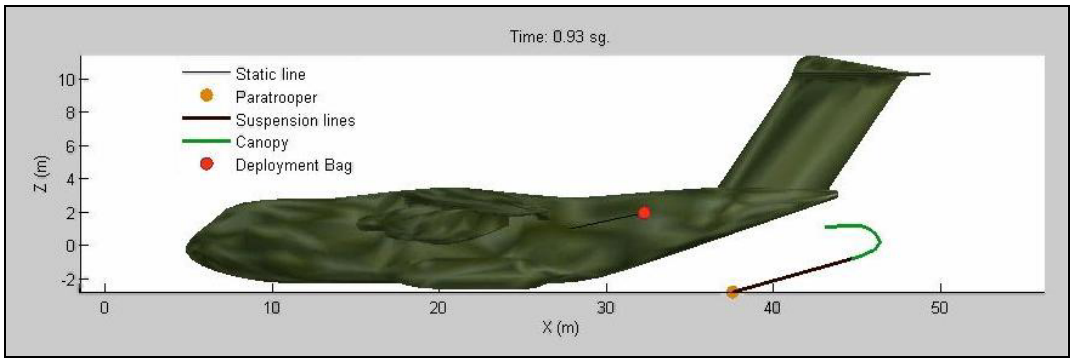

Figure 15: Cross flow effects phase (II)

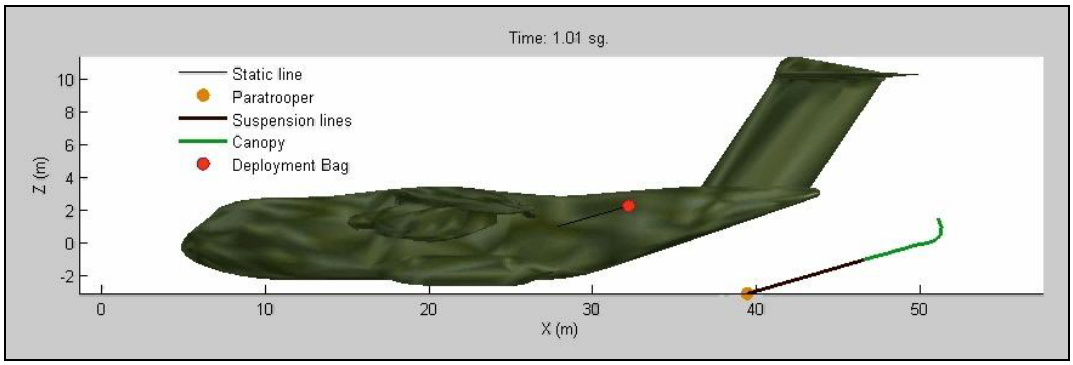

Figure 16: Cross flow effects phase (III)

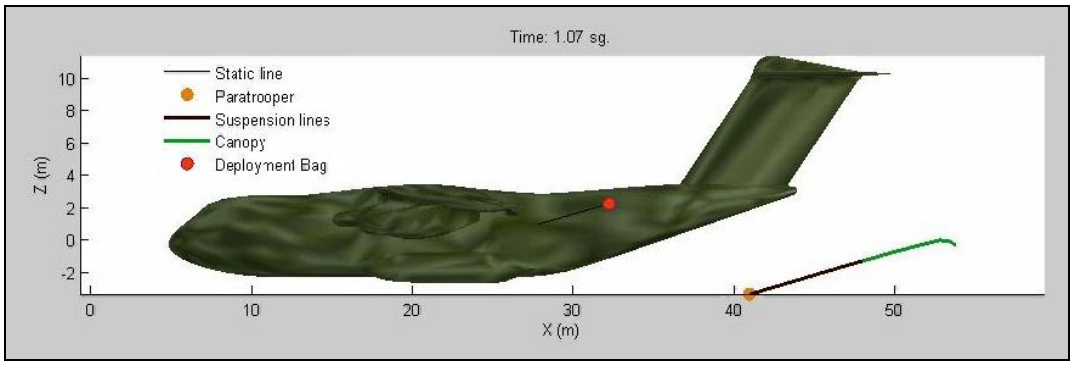

Figure 17: Start of inflation

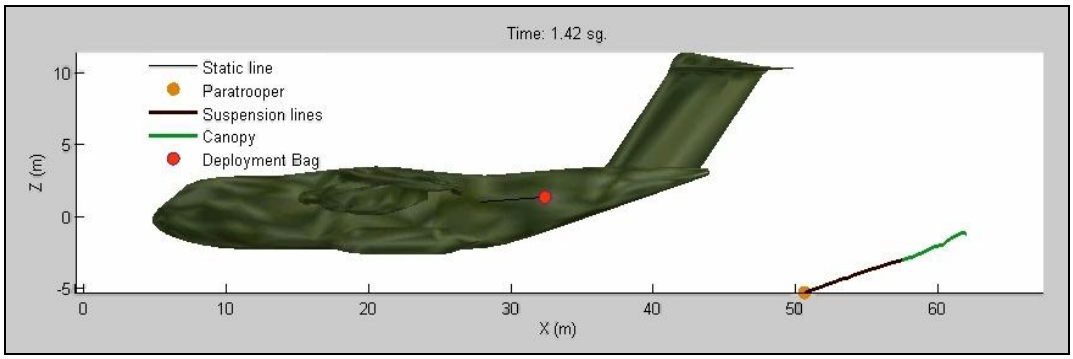

Figure 18: Inflation (I)

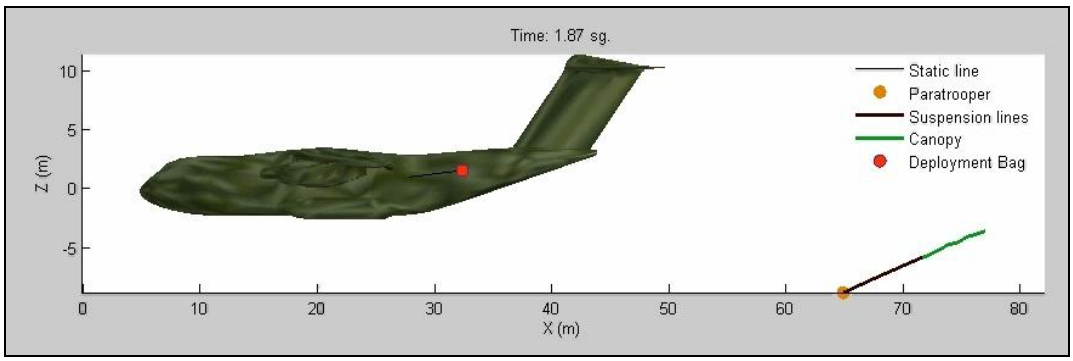

Figure 19: Inflation (II)

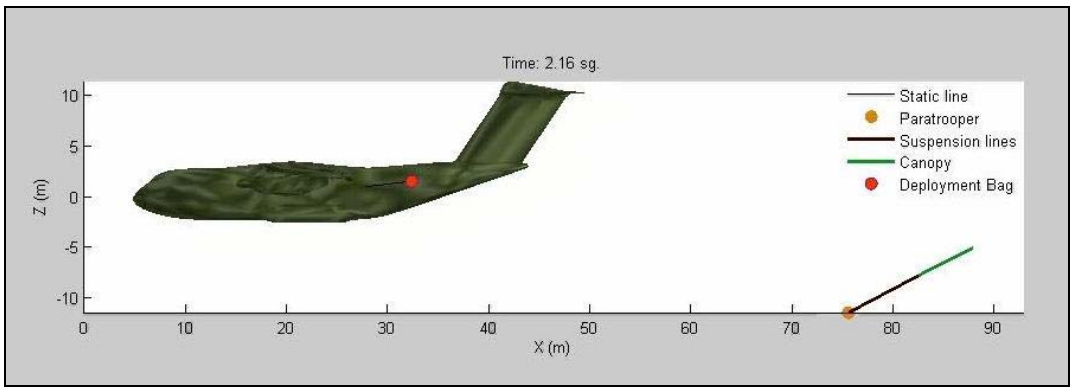

Figure 20: Inflation (III)

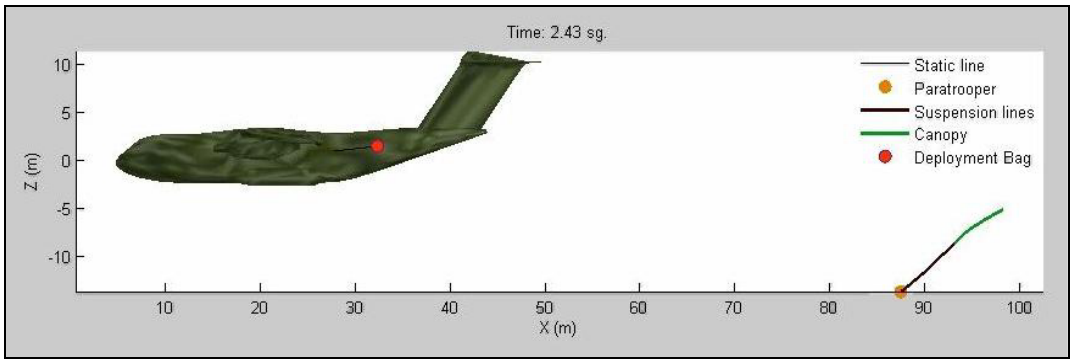

Figure 21: End of inflation

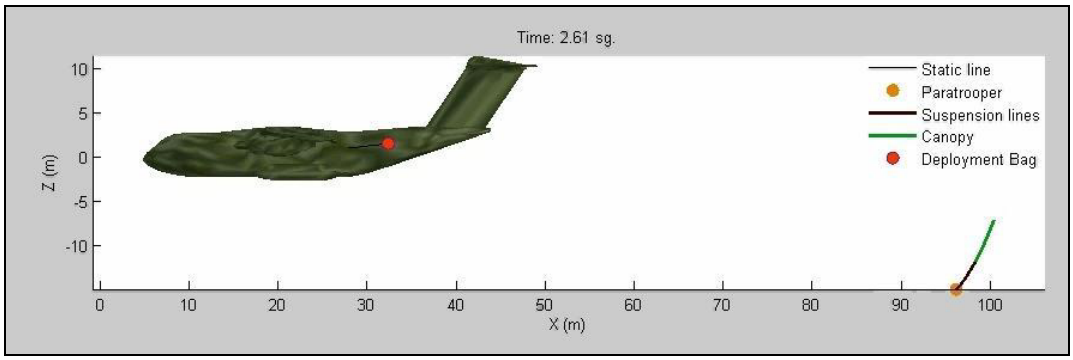

Figure 22: Descent and oscillation (I)

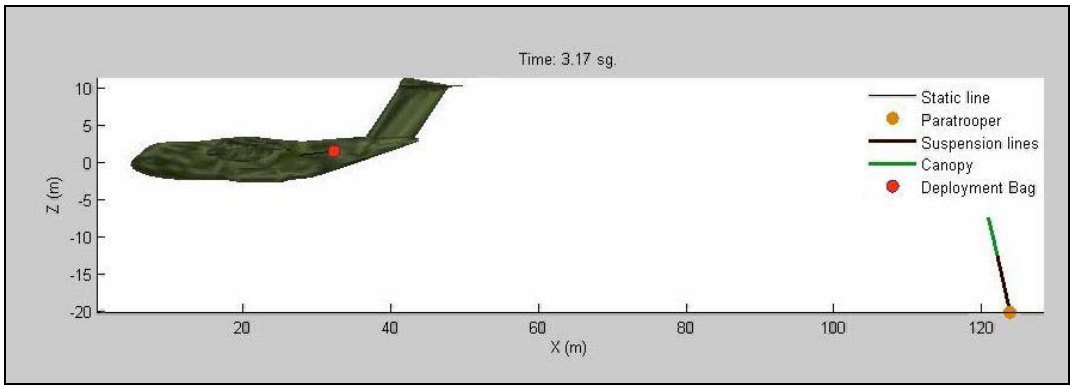

Figure 23: Descent and oscillation (II)

Due to the uncertainties in the values of some of the parameters used, the program was designed to permit Montecarlo simulations of the trajectories, allowing different probability distributions for each parameter. These Montecarlo simulations can be done for one isolated parameter, which permits a sensitivity study, or for a set of parameters, which permit to simulate a real paratrooper air delivery.

Figures 24 and 25 show the result of a hundred trajectories Montecarlo simulation having a variation of paratrooper mass (normal distribution with a mean value of 150 kg and $3\sigma = 50$kg).

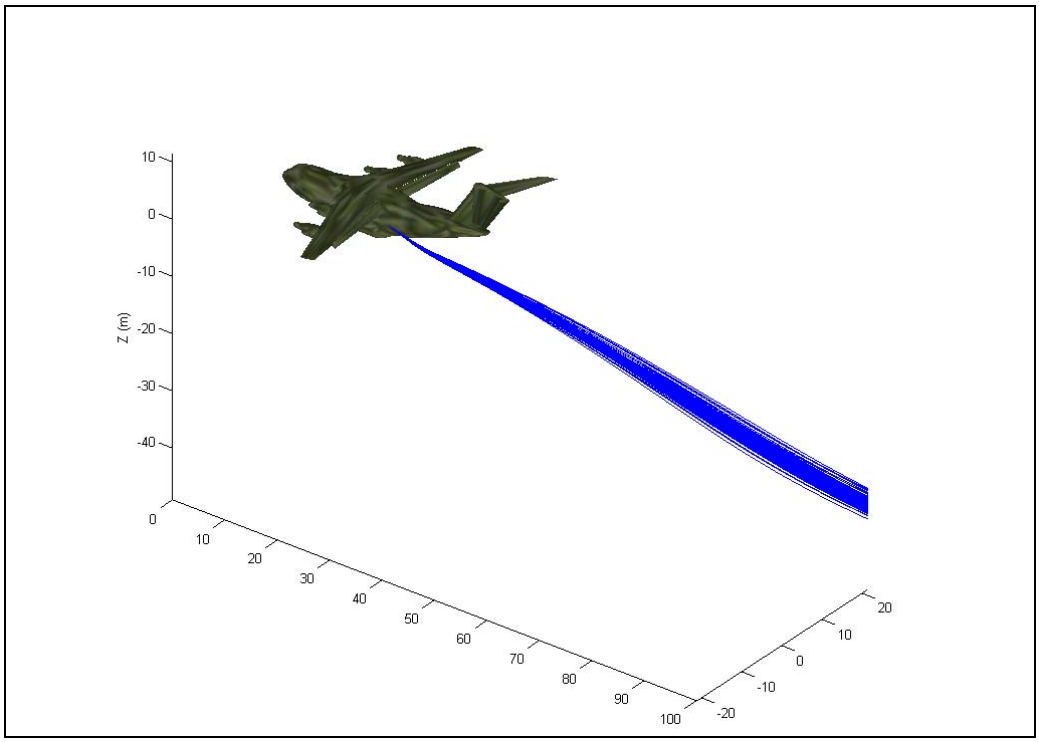

Figure 24: Montecarlo simulation for paratrooper mass parameter variation

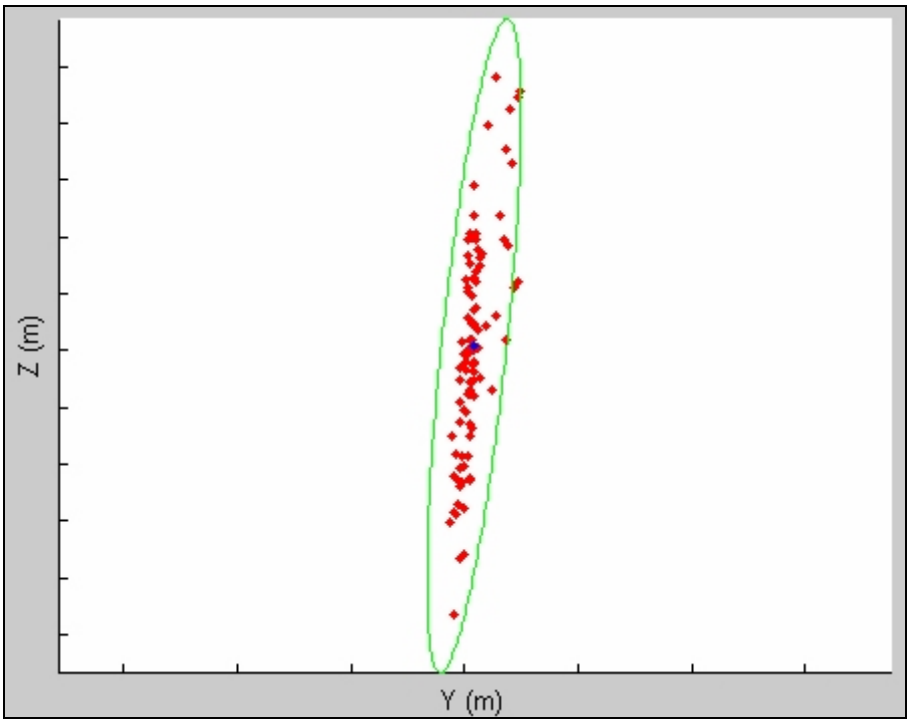

Figure 25: Intersections of trajectories on a X-constant plane for a Montecarlo simulation

6. CONCLUSIONS

A computer simulation with the capability to predict paratrooper deployment by static line is presented. The complete deployment process, from the moment when the paratrooper exits the aircraft to full canopy inflation and beyond, is split into three phases, which are tackled by different theoretical approaches.

Montecarlo simulations allow performing different statistical analysis, such as crossover probability, thus helping in determining the optimum condition for paratrooper mass delivery before the start of flight testing.

The initial results agree well with photographic and video data of actual paratrooper jumps. Further validation is on-going.

The tool is currently being used in the A400M development program.

7. REFERENCES

[1] Spong, E.D., Tavernetti, L.R., “Personnel Airdrop Optimization from Widebody Transports”, The Aerospace and Airport Technology Congress and Exhibition, Birmingham, UK, October 17-19, 1995.

[2] Kunz, S.E., “Analysis of Initial Parachute Deployment During Mass Assault”, 14th AIAA Aerodynamic Decelerator Systems Conference, AIAA 97-1351, San Francisco, June 2-6, 1997.

[3] Video of Paratrooper Airdrop from C-130H.

[4] Accorsi, M.L., Charles, R.D., Benney, R.J., “Computer Simulation and Evaluation of Static Line Deployment Procedures”, 18th AIAA Aerodynamic Decelerator Systems Conference, AIAA 2005-1631, 2005.

[5] Moog, R.D., “Aerodynamic Line Bowing During Parachute Deployment”, 5th AIAA Aerodynamic Deceleration Systems Conference, AIAA 75-1381, Albuquerque, New Mexico, November 17-19, 1975.

[6] J. W. Purvis, “Improved Prediction of Parachute Line Sail During Lines-First Deployment”, AIAA 84-0786, April 1984.

[7] Knacke, T.W., “Parachute Recovery Systems Design Manual”, Para Publishing, Santa Barbara, 1992.

[8] Kuethe, Arnold M., “Foundations of Aerodynamics”, John Wiley & Sons, Inc, 1986.

[9] Houghton E.L., Boswell R.P., “Further Aerodynamics for Engineering Students”, Edward Arnold, London, 1969, pp. 101-105.

[10] K. E. French, “Inflation of a Parachute”, AIAA Journal, Val.1, No.11, November 1963.

[11] Doherr, K.-F., “Extended Parachute Opening Shock Estimation Method”, 17th AIAA Aerodynamic Decelerator Systems Technology Conference and Seminar, AIAA 2003-2173, Monterey, California, May 19-22, 2003.

[12] Cockrell, D.J., “The Aerodynamics of Parachutes”, AGARDograph No.295, 1987.

SYMPOSIA DISCUSSION – PAPER NO: 3

Author's Name: F-J. Mariscal Sánchez

Discussor's Name: Scott Morton

Question:
1) Is the fluid volume input to the analysis tool static or time accurate?
2) Could you allow dynamic data?

Author's Response:
1) The flow field is "frozen". As only the lateral doors are open, the fluctuations on the flow field (like propeller induced fluctuations) are of much high frequency than paratrooper's dynamics. The dynamics of the paratroopers are taken into account by the relative motion of the paratrooper relative to the flow.
2) The model could be adapted to allow for dynamic data.

Discussor's Name: A. Bergmann

Question:
What is the idea for a proper validation of the CFD-method? What can be one in WTT testing and what has to be left for flight testing?

Author's Response:
For a validation of the trajectory simulation tool flight-testing would finally be needed, although there is space for WTT. In fact, the near flow field has been obtained by WTT. The first moments of the trajectory could be evaluated also in WTT. To adequately reproduce inflation phase in WTT seems very difficult, but if a scale parachute is properly modeled and characterized, it could be possible to check trajectory simulation tool against WTT results.

Discussor's Name: (no name given)

Question:
What method of computing the "segment" aerodynamic forces is useful?

Author's Response:
Aerodynamic forces in segments are divided in an axial component, caused by skin-friction drag, and a normal component modeled as cross-flow drag. Canopy and suspension lines are idealized as circular cylinders. Variation of aerodynamic parameters are also taken into account on Montecarlo simulations.

Discussor's Name: Major Lucy Giles

Question:
Have there been any significant design features on A400M that have been changed/altered as a result of the Flow Field Model work?

Author's Response:
So far, A400M shows no crossover tendency. However, different mitigations (lateral doors flow deflectors, landing gear doors opening, flap setting,… are being studied in case problems arise during flight tests.

Discussor's Name: M. Vallance

Question:
1) Is model mature to allow for prediction or airflow influence of defensive suite aerials/sensors?
2) Is model taking into account of proposed influence?

Author's Response:
1) As long as these sensors are big enough to influence the flow fields used in simulations (measured in wind tunnel or CFD), the model could predict its influence.
2) Yes, a powered model reproducing C_T was used for flow survey on wind tunnel tests.

Discussor's Name: I.I. Lipatov

Question:
You have mentioned inflation model. What does it mean SCd symbol? Can you evaluate an accuracy of the inflation model?

Author's Response:
$S.C_D$ is the "equivalent drag area". That is the aerodynamic drag divided by dynamic pressure.
Different papers can be found on the literature regarding the Pflanz-Ludtke inflation model. To take into account differences from this model, statistical variations of the parameters involved in inflation are considered on Montecarlo simulations.

Discussor's Name: Richard Benney

Question:
Did you vary the initial velocities of the jumper (mode)?

Author's Response:
Yes, varied initial velocity of jumper in both directions. Results (Montecarlo simulations) are included in the paper.